# Experimental Study on the Performance Enhancement of a Water Chiller

M.M. Alkhaja, M.R. Salem, K.M. Elshazly and M.F. Abdrabbo(*)
Mechanical Engineering Department, Faculty of Engineering at Shoubra, Benha University, 108 Shoubra St., 11629, Cairo, Egypt
(*)Corresponding author (M.F. Abdrabbo): Tel: +201223949093 & Email: fayek44@yahoo.com

**Abstract**
This work experimentally investigates the effect of the geometrical parameters of a vertical helically coiled tube in tube (HCTIT) evaporator on the coefficient of performance (COP) of a vapour compression refrigeration system (VCRS) used as a water chiller. Five HCTIT evaporators through which R134a flows in the internal tube, are constructed and tested at different flow rates of the heating water in their annulus. They are geometrically divided into two groups; the first group is fabricated such that the internal tube curvature ratios ($\delta_{ev,i}$) is varied from 0.0238 to 0.0334 while the other group represents another three-different coil torsions ($\lambda$) from 0.0522 to 0.0948. The results show that the COP of the VCRS is enhanced with decreasing $\delta_{ev,i}$, increasing $\lambda$, and increasing the condenser to evaporator pressures ratio. Finally, an experimental correlation is developed to predict the COP of the VCRS.

**Keywords:** Helically coiled tube, Evaporator, Water chiller, Curvature, Torsion, Performance.

## 1. Introduction

The VCRS is one of the refrigeration systems, which is used in most domestic refrigerators in addition to in numerous large industrial and commercial refrigeration systems. This system consists of four main components; compressor, condenser, capillary tube, and evaporator. The condenser and evaporator are responsible to transfer the heat energy from/to the refrigerant. Therefore, enhancing their heat transfer rate will enhance the COP of the refrigeration system.

To achieve the desired heat transfer rate in the given design and size of the heat exchanger at an economic pumping power, numerous techniques have been proposed. These enhancement techniques can be categorized as active and passive techniques [1–6].

Helically coiled tubes (HCTs) are widely used as heat exchangers and have applications as heating systems, chilled water systems, ground water systems and residential use. These utilizations are common in various industries: chemical, biological, petrochemical, mechanical, biomedical and others. This wide application of the HCTs is due to their compactness and the geometry promotes good mixing of the fluids, which leads to increasing the heat transfer coefficients [6, 7]. Due to the extensive use of the HCTs in these applications, knowledge about the heat transfer and pressure drop characteristics are very important.

A schematic representation of HCT characteristics with main geometrical parameters is shown in Fig. 1. Considering any cross section of the HCT created by a plane passing through the coil axis, the side of tube wall nearest to the coil axis is termed inner side of the coil, while the farthest side is labelled as outer side of the coil. The HCT can be geometrically described by the followings:

- $S$ Coil spacing; it is the minimum distance between two adjacent turns from surface to surface,
- $p_c$ Coil pitch; it is the distance between two adjacent turns from centre to centre, $p_c = S + d_{t,o}$
- $d_{t,o}$ Outer diameter of the HCT
- $D_{c,i}$ Inner diameter of the coil curvature
- $D_c$ Mean diameter of the coil curvature, $D_c = D_{c,i} + d_{t,o}$
- $D_{c,o}$ Outer diameter of the coil curvature, $D_{c,o} = D_c + d_{t,o}$
- $N$ Number of the turns of the HCT
- $L_c$ Coil length, $L_c = (N * p_c) + d_{t,o}$
- $L_t$ HCT length, $L_t = N\pi D_c$

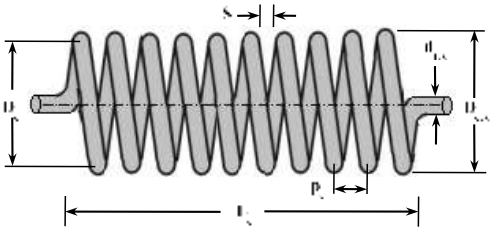

**Fig. 1: Basic geometry of a HCT.**

There are also dimensionless parameters that were commonly used to explain the effects of the coil curvature and coil torsion. They are defined as follows [6, 7]:

$$\delta = d_{t,i}/D_c \quad (1)$$

$$\lambda = p_c/\pi D_c \quad (2)$$

Where $\delta$ is coil curvature ratio, while $\lambda$ is coil torsion (pitch ratio).

Venkataramanamurthy and Senthil [8] carried out an experimental study for the comparisons of energy, exergy flow and second law efficiency of R22 and its substitutes R-436b in VCRS. The investigations presented the effects of the evaporating temperatures on the exergy flow losses and second law efficiency and COP of the VCRS. Reddy et al. [9] did a numerical analysis of VCRS using R134a, R143a, R152a, R404A, R410A, R502 and R507A and discussed the effect of evaporator temperature, degree of subcooling at condenser outlet, superheating of evaporator outlet, vapour liquid heat exchanger effectiveness and degree of condenser temperature on COP and exergetic efficiency. They reported that evaporator and condenser temperature have significant effect on both COP and exergetic efficiency and also found that R134a has the better performance while R407C has poor performance. Soni and Gupta [10] performed an exergy analysis for

theoretical VCRS using R404A, R407C and R410A. They developed equations of exergetic efficiency, exergy destruction for the main components of VCRS in addition to an expression for COP of VCRS. The relations for total exergy destruction in the system, the overall exegetic efficiency of the system and exergy destruction ratio related to exergetic efficiency were obtained. Mula and Harish [11] carried out an experimental analysis on VCRS with R134a. A diffuser has been introduced in between compressor and condenser so that power input to the compressor has been reduced there by enhancing COP. Rakesh et al. [12] carried out experimental and numerical analysis on a VCRS with R134a. In the VCRS, a diffuser has been introduced in between the compressor and condenser so that the power input to the compressor has been reduced there by enhancing COP by 31%. Gilla and Singh [13] carried out an experimental investigation with R134a and LPG refrigerant mixture (composed of R134a and LPG in the ratio of 28:72 by weight) as an alternative to R134a in a VCRS. Performance tests were performed under different evaporator and condenser temperatures with controlled ambient conditions. The results showed that the R134a and LPG refrigerant mixture has a higher COP and lower compressor discharge temperature and pull down time as compared to R134a by about 15.1–17.8%, 2.1–13.9% and 1–5.9%, respectively.

Yu et al. [14] presented an experimental study on the condensation heat transfer of R134a flowing inside a HCT with cooling water flowing in annulus. It was indicated that the heat transfer characteristics was significantly affected by the orientation of the helical pipe. Murai et al. [15] used the backlight imaging tomography to examine the centrifugal acceleration of phase distribution and interfacial pattern for gas–liquid two-phase flow in a HCT. The results showed that the centrifugal force resulting from the curvature of coil generated a wall-clinging liquid layer against gravity. This caused the interfacial area to be enhanced for the high superficial velocity. Naphon and Wongwises [16] provided a survey on the characteristics of heat transfer, and single and two-phase flow in coiled tubes. They concluded that the performance of the heat exchangers being improved, the heat transfer enhancement decreased the size of the heat exchanger. Ness [17] presented experimental data on the average heat transfer coefficients for four annular-coil geometries, covering the laminar, transition and turbulent flow regimes. The results showed that the heat transfer in the laminar and transition regions significantly enhanced with increasing the coil curvature. While this enhancement was smaller in the turbulent flow regime. Colorado et al. [18] performed a numerical simulation and experimental validation of a HCTIT vertical condenser. The condenser uses water as a working fluid connected in counter current. It was revealed that changing the mass flow rate in the internal tube makes a significant variation of the condensation pressure and temperature. Ahmed [19] experimentally and theoretically investigated the flow boiling of refrigerant R134a in small diameter HCTITs for the evaporator of tiny refrigeration systems. It was shown that decreasing the tube diameter and increasing the coil curvature enhance the boiling heat transfer coefficient by 58% and 130%, respectively. Nada et al. [20] experimentally investigated the performance of helically coiled multi tubes-in-tube heat exchanger. The experiments demonstrated that coils with three inner tubes provides the highest values of heat transfer coefficient and compactness parameter. Mhaske and Palande [21] experimentally and numerically investigation a counter flow HCTIT heat exchanger with a wire wound over the inner tube. It was demonstrated that the overall heat transfer coefficient of the wire winding HCTIT heat exchanger was more as compared to the conventional heat exchanger.

## 2. Experimental Apparatus

The apparatus used in the present investigation comprises heating and cooling water loops in addition to the refrigerant circuit. The hot water (supplied to the VCRS evaporator-annulus) circuit consists of a heating unit with a thermostat, pump, valves, water flow meter and the connecting pipes. While the cooling water supplied to the VCRS condenser-annulus from the local water supply is passed through the connecting pipes and is controlled by a valve and water flow meter. The refrigerant (R134a) circuit consists of a compressor, valves, HCTIT condenser, filter drier, sight glass, capillary tube, HCTIT evaporator, temperature sensors, pressure/pressure difference transducers and the connecting pipes. Fig. 2 is a schematic diagram of the experimental setup.

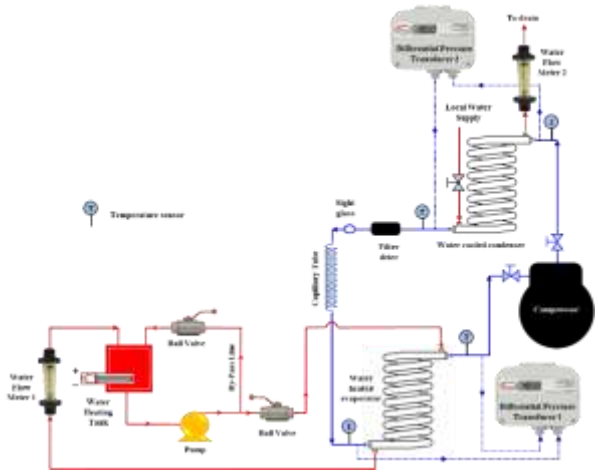

**Fig. 2: Schematic diagram of the experimental setup.**

Six HCTIT heat exchangers of counter-flow configuration are constructed. Five of them are with different curvature ratios and torsions; used as evaporators. The characteristic dimensions of the different configurations are revealed in Table 1. In the experimental runs, HCTs no. 1 to 5 are used as evaporators while HCT no. 2 is used as a condenser. The HCTITs are formed from straight soft copper tubes of the same length 6000 mm. The inner tube is of 9.53 mm external diameter and 8.31 mm internal diameter, while the outer tube is of 19.05 mm external diameter and 17.93 mm internal diameter. The five HCTITs are divided into two groups; three HCT-curvatures with the same coil torsion, while the other group represents another three different HCT-torsions with the same curvature ratio. To investigate the effect of coils

geometry ($\delta, \lambda$), all HCTs have the same heat transfer area where $L_t$, $d_{t,i}$ and $d_{t,o}$ are the same for all coils. It should be noted that for HCTs with the same torsion (HCTs no. 1 to 3), as $D_c$ decreases, $p_c$ must decrease. In addition, the number of coil turns must increase due to the fixed length of the tube as illustrated in Table 1.

**Table 1: Characteristic dimensions of the tested coils.**

| HCT no. | $D_{c,i}$ (mm) | δ | S (mm) | $p_c$ (mm) | λ | $L_c$ (mm) | N |
|---|---|---|---|---|---|---|---|
| | Inner Tube | | | | | | |
| 1 | 239.5 | 0.0334 | 48.0 | 57.51 | 0.0735 | 570 | 9.6 |
| 2 | 289.5 | 0.0278 | 59.5 | 69.05 | | | 8.0 |
| 3 | 339.5 | 0.0238 | 71.1 | 80.59 | | | 6.8 |
| 4 | 289.5 | 0.0278 | 39.5 | 49.05 | 0.0522 | 411 | 8.0 |
| 2 | | | 59.5 | 69.05 | 0.0735 | 570 | |
| 5 | | | 79.5 | 89.05 | 0.0948 | 730 | |
| 8 | 289.5 | 0.0278 | 59.5 | 69.05 | 0.0735 | 570 | 8.0 |

To prevent any flattening to the HCTs during coiling process, the tubes are filled with fine sand before bending to preserve the smoothness of the inner surface and this is washed with hot water after the process. Furthermore, care is taken to locate the inner tube into the centre of the outer tube by using circular ring that have the dimension of the annulus with a clearance of 0.5 mm during the filling process. As the annulus is filled with fine sand, the ring is moved systematically until it exits from the other side of the tube after the annulus is fully filled with the fine sand. Moreover, outer surface of the HCTIT evaporators/condensers is thermally isolated with thick insulation using a rubber insulation material.

In the present cycle, a 1 hp centrifugal compressor model is used. The used capillary device is a narrow copper tube of 0.64 mm internal diameter, and 1500 mm effective length. The capillary tube is coiled with internal coil diameter of 50 mm. Two digital pressure/differential pressure transducers are employed for measuring the pressure of the refrigerant at evaporator and condenser inlets and outlets. One of them is of a high scale (installed at the inlet and exit of the condenser) with a differential pressure range of 0–206.8 kPa, with maximum pressure of 17.24 bar. While the other transducer of a lower scale (installed at the inlet and exit of the evaporator) with a differential pressure range of 0–103.4 kPa, with maximum pressure of 3.45 bar. Both transducers are of accuracy of ±1% of full scale.

Four digital temperature sensors, with a resolution of 0.1°C are used to measure the temperatures of the refrigerant entering or leaving the evaporator and the condenser. These sensors are conducted on the outer surface of the copper tube. Neglecting the thermal resistance of the tube wall, the temperature readings are assumed to be equal to the refrigerant temperatures at these locations. In the present experiment setup, soft copper tubes of 9.53 mm external diameter and 8.31 mm internal diameter are used for all connections. Furthermore, four copper T-shaped connectors are used to connect the pressure transducers. Moreover, to prevent any effect of the surroundings conditions, the outer surface of all copper connections is thermally isolated with thick insulation using a rubber insulation material. It should be noted that all copper piping are thermally insulated with using

Two electric heaters of a maximum power rating of 6 kW are fixed horizontally at the bottom of an insulated 50 liter heating tank to heat the water to the required temperature. The operation of the electric heaters is based on a pre-adjusted digital thermostat, which is used to keep a constant temperature of the water directed to the evaporator. There are three ports in the tank; two of them are in the top side of the tank, which represent the inlet ports from the evaporator and from the by-pass line. The other port is in the bottom, which represents the exit port to the pump.

Two identical variable area flow meters, 1.8–18 l/min flow rate range, are used to measure the volume flow rates of the heating and cooling water required for the evaporator and condenser, respectively. According to the manufacturer's data sheet, these meters are with accuracy of ±5% of reading. Four digital temperature sensors, with resolution of 0.1°C, are directly inserted into the flow streams, at approximately 50 mm from inlet and exit ports of the annulus of the evaporator and condenser, to measure the water inlet and outlet temperatures.

## 3. Experimental Procedures

To initiate the experiments, the following parts are assembled: the evaporator, compressor, condenser, filter drier, sight glass, capillary tube, heating tank, pump, water flow meters, piping, and the pressure transducers. These parts are connected together using either nuts or welding the pipes with silver solder. Then, the temperature sensors are attached at the inlet and outlet of the annulus side of the evaporator and condenser, in addition to on the refrigeration piping at evaporator and condenser inlets and outlets. After attaching the temperature sensors on the refrigerant tubes, they are well isolated from the surroundings. After assembling the VCRS components, it is charged with R134a.

The first step to collect the data from the system is to fill the heating tank with water from the domestic water supply, then the electric heaters are turned on. While the condenser annulus is linked to a tap of the domestic water supply through a flexible hose. Then the compressor and the pump are turned on. The temperature of the water entering the evaporator annulus (20±0.5°C) is adjusted by regulating the temperature of the heating tank through its thermostat. The water from the heating tank is circulated in the main line to the evaporator annulus at different flow rate in each experiment as revealed in Table 2. The remainder from the pumped flow is returned to the tank through a bypass line.

**Table 2: Range of operating conditions.**

| Parameters | Range or value |
|---|---|
| Evaporator heating water flow rate, l/min | 6.02–16.3 |
| Evaporator heating water inlet temperature, °C | 20 |
| Evaporator refrigerant Pressure, bar | $1.5 \le P_{ev} \le 2.1$ |
| Condenser cooling water flow rate, l/min | 8.08 |
| Condenser cooling water inlet temperature, °C | 28 |
| Condenser refrigerant Pressure, bar | $9.3 \le P_c \le 10.6$ |
| Condenser to evaporator pressure ratio | $5.1 \le P_c/P_{ev} \le 6.2$ |

## 4. Data Reduction

The measured temperatures and pressures during the experiments are used to calculate the specific enthalpy

of the refrigerant in the different locations of the VCRS. Microsoft Excel sheets are prepared to process the experimental data for the COP and the other characteristic parameters of the VCRS. The specific enthalpy of the refrigerant is estimated using its measured pressure and temperature at evaporator and condensers inlet end exit. The estimated specific enthalpies are used for calculating the following parameters:

$$RE = h_1 - h_4 \quad (3)$$

$$w_c = h_2 - h_1 \quad (4)$$

$$q_c = h_2 - h_3 \quad (5)$$

$$COP = RE/w_c = (h_1 - h_4)/(h_2 - h_1) \quad (6)$$

Where subscript 1 and 2 refer to the refrigerant at compressor inlet and exit, respectively, while 3, 4 refer to the refrigerant at capillary tube inlet an exit, respectively.

## 5. Results and Discussions

### 5.1 Effect of Evaporator Curvature

In this analysis, the three HCTs no. 1, 2 and 3 shown in Table 1 are considered as evaporators, while HCT no. 6 is used as a condenser. The evaporators are of inner tube curvature ratios of 0.0238 to 0.0334, and of the same torsion; λ = 0.0735. The operating conditions are varied according to Table 2. Figs. 3 to 9 present the obtained results.

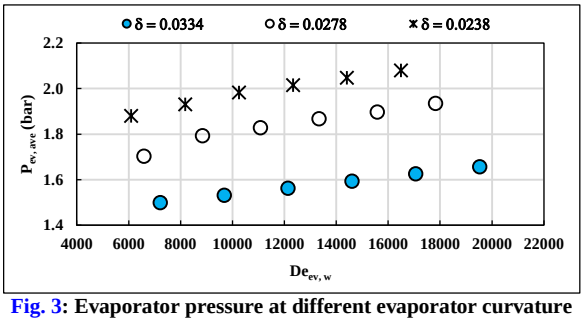


**Fig. 3: Evaporator pressure at different evaporator curvature ratios.**

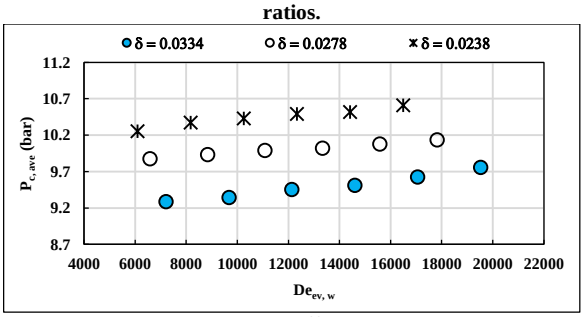


**Fig. 4: Condenser pressure at different evaporator curvature ratios.**

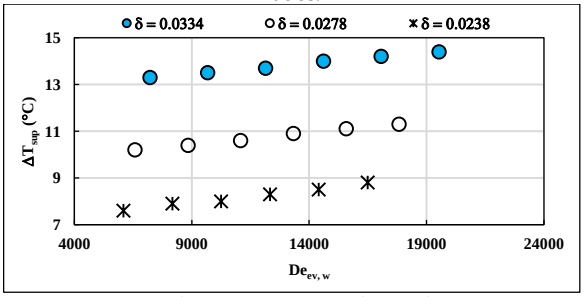


**Fig. 5: Amount of the superheating of the refrigerant in the evaporator at different evaporator curvature ratios.**

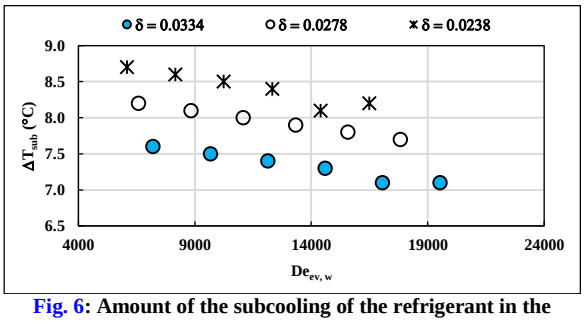


**Fig. 6: Amount of the subcooling of the refrigerant in the condenser at different evaporator curvature ratios.**

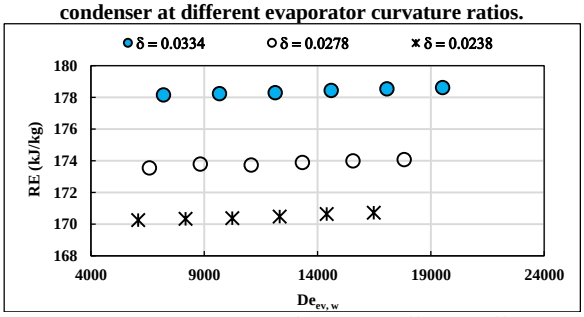


**Fig. 7: HCTIT evaporator refrigeration effect at different evaporator curvature ratios.**

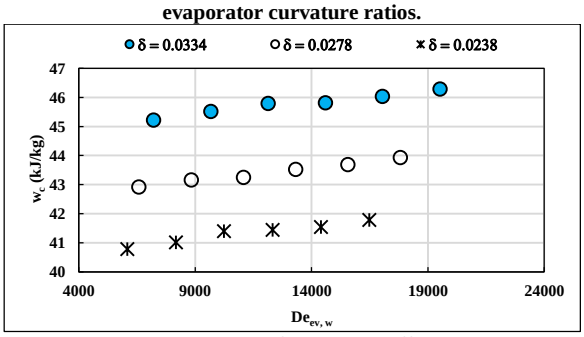


**Fig. 8: The compressor specific work at different evaporator curvature ratios.**

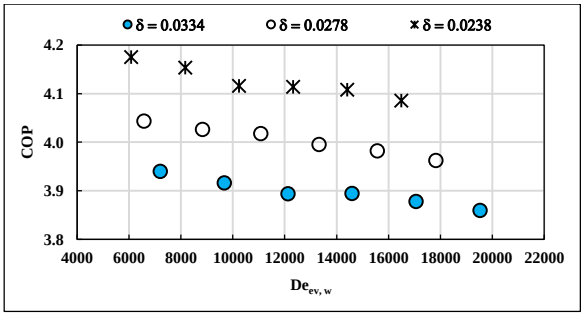


**Fig. 9: VCRS coefficient of performance at different evaporator curvature ratios.**

It is revealed that increasing the curvature ratio of the HCTIT evaporator leads to a significant decrease in the average pressures of the evaporator and the condenser, and in the refrigerant subcooling inside the condenser, in addition to a noticeable increase in the superheating of the refrigerant inside the evaporator. With increasing the curvature ratio of the internal tube of the HCTIT evaporator from 0.0238 to 0.0334, the evaporator average pressure decreased from 2 bar to 1.58 bar, respectively, while the condenser average pressure is decreased from 10.44 bar to 9.5 bar, respectively. In addition, the refrigerant is superheated inside the evaporator and subcooled inside the condenser by average values of 8.2°C and 8.4°C, respectively, at δ = 0.0238 and by 13.9°C and 7.3°C, respectively, at δ = 0.0334. This can be attributed to increasing the

centrifugal force with increasing evaporator curvature ratio, which induces more effective secondary flow. This reduces the compressor suction pressure, and consequently reduces the cycle pressures. This leads to decreasing their corresponding saturation temperatures, in addition to a higher superheating temperature of the refrigerant entering the condenser with increasing the evaporator curvature ratio. This slightly minimizes the subcooling of the refrigerant inside the condenser.

It is evident that these conditions affect the VCRS performance parameters as illustrated in Figs. 7 to 9. Increasing the curvature ratio of the internal tube of the HCTIT evaporator from 0.0238 to 0.0334 increases both the RE and the compressor specific work with an average percentage increase of 4.6% and 10.8%, respectively. This reduces the coefficient of the performance of the VCRS by an average percentage decrease of 5.5%. As mentioned before, this is due to increasing the centrifugal force in both sides of the HCTIT evaporator with increasing the coil curvature ratio, which induces more effective secondary flow. Therefore, the refrigerant superheating inside the evaporator increases, which enhances the evaporator refrigeration effect, while at the same time, the specific volume of the refrigerant at the compressor inlet increases, and consequently the specific work required to compress the refrigerant molecules increases.

Moreover, the water Dean Number in the HCTIT evaporator annulus slightly affect the compressor specific work and is nearly negligible on the RE, and consequently slightly affects the COP of the cycle. This is due to increasing the superheating of the refrigerant inside the evaporator and at the same time, the subcooling in the condenser slightly decreases with increasing the water Dean Number in the HCTIT evaporator-annulus. This diminishes its effect on the RE. While the compressor specific work increases as a result of increasing the specific volume of the refrigerant at the compressor inlet due increasing the refrigerant superheating with increasing water Dean Number. Therefore, the COP of the VCRS decreases.

### 5.2 Effect of Evaporator Torsion

In this analysis, the three HCTs no. 4, 2 and 5 shown in Table 1 are considered as evaporators, while HCT no. 6 is used as a condenser. The evaporators are of torsions of 0.0522 to 0.0948, and of the same inner tube curvature ratio; $\delta = 0.0278$. The operating conditions are varied according to Table 2. Figs. 10 to 16 present the obtained results.

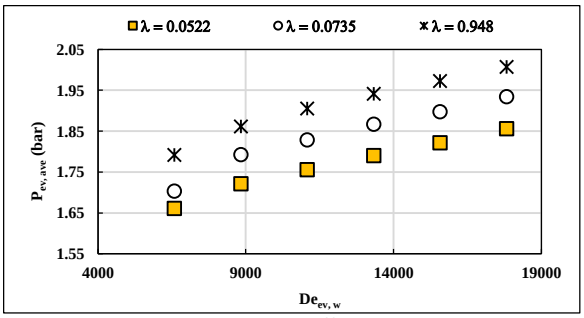


**Fig. 10: Evaporator pressure at different evaporator torsions.**

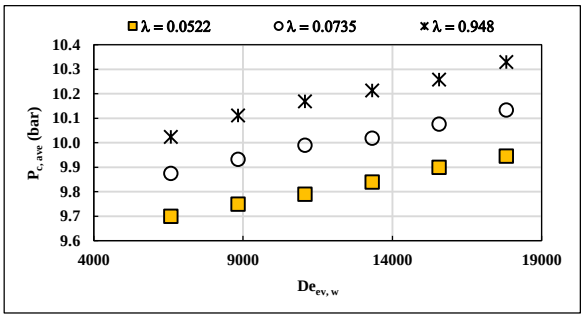


**Fig. 11: Condenser pressure at different evaporator torsions.**

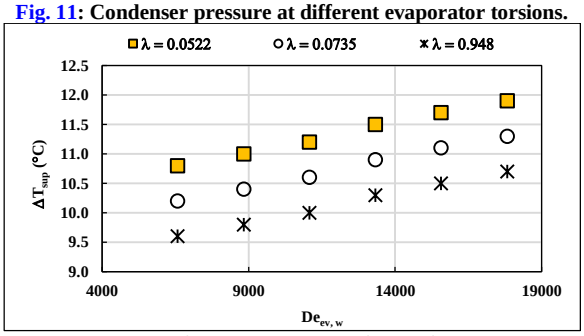


**Fig. 12: Amount of the superheating of the refrigerant in the evaporator at different evaporator torsions.**

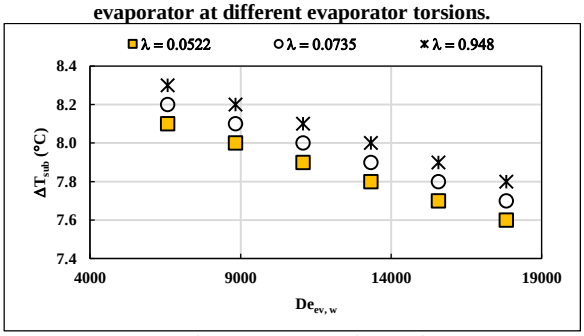


**Fig. 13: Amount of the subcooling of the refrigerant in the condenser at different evaporator torsions.**

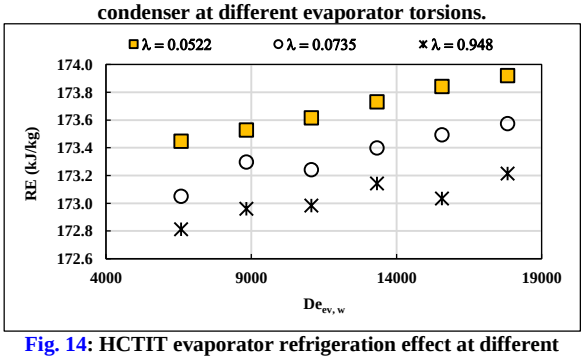


**Fig. 14: HCTIT evaporator refrigeration effect at different evaporator torsions.**

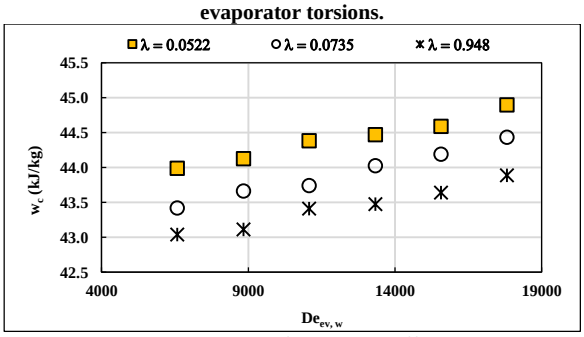


**Fig. 15: The compressor specific work at different evaporator torsions.**

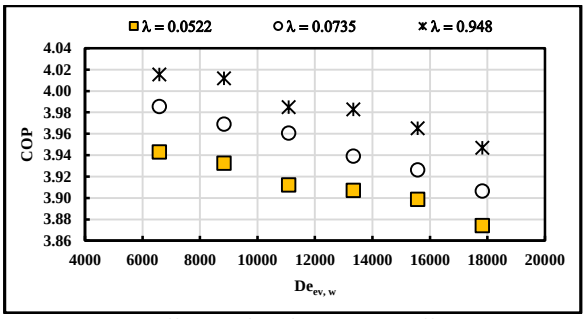


**Fig. 16: VCRS coefficient of performance at different evaporator torsions.**

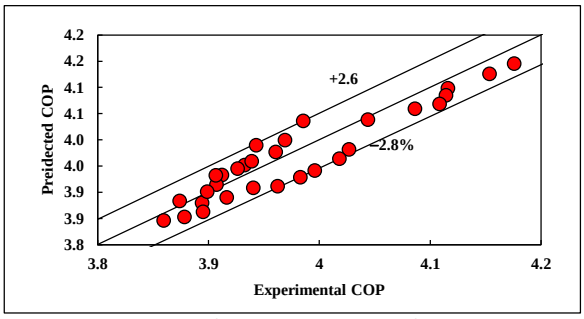


**Fig. 17: Comparison of experimental values for COP with that correlated by Eq. (7).**

It is observed that the effect of coil torsion is lower than that of the coil curvature ratio in the investigated range of these parameters. It is clear that increasing the HCTIT evaporator torsion slightly increases the average pressures of the evaporator and condenser, in addition to the refrigerant subcooling inside the condenser, and slightly reduces the superheating of the refrigerant in the evaporator. With increasing the torsion of the HCTIT evaporator from 0.0522 to 0.0948, the evaporator average pressure increased from 1.77 bar to 1.91 bar, respectively, while the condenser average pressure is decreased from 9.82 bar to 10.18 bar, respectively. In addition, the refrigerant is superheated inside the evaporator and subcooled inside the condenser by average values of 11.4°C and 7.9°C, respectively, at $\lambda$ = 0.0522 and by 10.2°C and 8.1°C, respectively, at $\lambda$ = 0.0948. This can be returned to increasing the rotational force as a result of increasing the coil torsion which diminishes the secondary flow that established by the centrifugal effect.

It is clear that these conditions slightly affect the VCRS performance parameters as illustrated in Figs. 14 to 16. It is clear that increasing the HCTIT evaporator torsion from 0.0522 to 0.0948 slightly decreases both the RE and the compressor specific work with an average percentage decrease of 0.4% and 2.2%, respectively. This slightly enhances the COP of the VCRS by an average percentage decrease of 2%. As mentioned before, increasing the evaporator torsion slightly reduces the refrigerant superheating inside the evaporator, which slightly minimizes the evaporator refrigeration effect. While at the same time, the specific volume of the refrigerant at the compressor inlet decreases, and consequently the specific work required to compress the refrigerant molecules decreases.

## 6. Correlation for the COP of the VCRS

Using the present experimental data, a correlation was developed to predict the COP of the VCRS as a function in the HCTIT evaporator curvature ratio and torsion in addition to the cycle pressure ratio as follows;

$$COP = 0.912\ \delta_{ev,i}^{-0.292}\ \lambda_{ev}^{0.042}\left(\frac{P_c}{P_{ev}}\right)^{0.314} \qquad (7)$$

Eq. 7 is applicable for a VCRS with HCTIT evaporator of $0.0238 \le \delta_{ev,i} \le 0.0334$, $0.0522 \le \lambda_{ev} \le 0.0948$, $1.5\ \text{bar} \le P_{ev} \le 2.1\ \text{bar}$, $9.3\ \text{bar} \le P_c \le 10.6\ \text{bar}$, and $5.1 \le (P_c/P_{ev}) \le 6.2$. A comparison of the experimental COP with that calculated by the proposed correlation is shown in Fig. 17.

From this figures, it is evident that the proposed correlation is in good agreement with the present experimental data. It is clearly seen that the data falls of the proposed equations within maximum deviation of $\pm 2.8\%$.

## 7. Summary

From the previous sections and according to the results obtained using the experimental investigation, the following conclusions can be expressed:

- Increasing the HCTIT evaporator curvature ratio reduces the COP of the VCRS.
- Increasing the HCTIT evaporator torsion increases the COP of the VCRS.
- Increasing the condenser to evaporator pressures ratio enhances the COP of the VCRS.
- Experimental correlation is developed to predict the COP of the VCRS.

**References**


[1] Jin Yang, Hugues Rivard, and Radu Zmeureanu, "Building Energy Predication with Adaptive Artificial Neural Networks", Ninth International IBPSA Conference Montréal, August 15–18, 2005.

[2] Guy Cheron, Françoise Leurs, Ana Bengoetxea, Ana Maria Cebolla, Jean-Philippe Draye, Pablo D'alcantara, and Bernard Dan, "Biological Signals Identification by a Dynamic Recurrent Neural Network: from Oculomotor Neural Integrator to Complex Human Movements and Locomotion", Chapter 2, Recurrent Neural Networks, book edited by Xiaolin Hu and P. Balasubramaniam, September 1, 2008.

[3] Anil K. Jain, Jianchang Mao, and K.M. Mohiuddin, "Artificial Neural Networks: A Tutorial", IEEE Computer, vol. 29(3), pp.31-44, March 1996.

[4] Maitha H. Al Shamisi, Ali H. Assi and Hassan A. N. Hejase, "Using MATLAB to Develop Artificial Neural Network Models for Predicting Global Solar Radiation in Al Ain City – UAE", Engineering Education and Research Using MATLAB, Dr. Ali Assi (Ed.), ISBN: 978-953-307-656-0, InTech, pp. 219–238, October 2011.

[5] F. Tymvios, S. Michaelides, and C. Skouteli, "Estimation of Surface solar radiation with Artificial neural networks", In: Modeling Solar Radiation at the Earth Surface, Viorel Badescu, Springer, Germany, ISBN 978-3-540-77454-9, pp. 221–256, 2008.

[6] M.R. Salem, R.K. Ali, R.Y. Sakr, and K.M. Elshazly, "Experimental Study on Convective Heat Transfer and Pressure Drop of Water-Based Nanofluid inside Shell and Coil Heat Exchanger",

PhD dissertation, Faculty of Engineering at Shoubra, Benha University, 2014. DOI: 10.13140/RG.2.2.31958.75846.

[7] R. Gupta, R.K. Wanchoo and T.R.M.J. Ali, "Laminar Flow in Helical Coils: A Parametric Study", Industrial & Engineering Chemistry Research, vol. 50(2), pp. 1150–1157, 2011.

[8] V. P. Venkataramanamurthy and P. Senthil Kumar, "Experimental Comparative Energy, Exergy Flow and Second Law Efficiency Analysis of R22, R436b Vapour Compression Refrigeration Cycles", International Journal of science and Technology, vol. 2(5), pp. 1399-1412, 2010.

[9] V. Siva Reddy, N.L. Panwar, S.C. Kaushik, "Exergy analysis of a vapour compression refrigeration system with R134a, R143a, R152a, R404A, R407C, R410A, R502 and R507A", Int. Journal of .Clean Techn Environ Policy, vol. 14, pp. 47-53., 2012.

[10] Jyoti Soni and R. C. Gupta, "Performance analysis of vapour compression refrigeration system with R404A, R407C and R410A", International Journal of Mechanical Engineering and Robotics Research, vol. 2(1), pp. 25-36, 2013.

[11] Venkata Ramana Reddy Mula, H.V. Harish, "Enhancement of coefficient of performance in vapour compression refrigeration cycle", International Journal of Research in Aeronautical and Mechanical Engineering, vol. 3(10), pp. 49-62, 2015.

[12] R. Rakesh, H. N. Manjunath, R. Krupa, Sushanth H. Gowda, Kiran Aithal S , "A Study on Enhancing COP in VCR by Providing Diffuser in between Condenser and Compressor", Energy and Power, vol. 7(5), pp. 142–148, 2017.

[13] Jatinder Gilla and Jagdev Singh, "Energy Analysis of Vapor Compression Refrigeration System Using Mixture of R134a and LPG as Refrigerant", International Journal of Refrigeration, vol. 84, pp. 287–299, 2017.

[14] B. Yu, J.T. Han, H.J. Kang, C.X. Lin, A. Awwad, M.A. Ebadian, "Condensation Heat Transfer of R-134a Flow inside Helical Pipes at Different Orientations", Int. Commun. Heat Mass Transfer, vol. 30, pp. 745–754, 2003.

[15] Y. Murai, H. Oiwa, T. Sasaki, K. Kondou, S. Yoshikawa, F. Yamamoto, "Backlight Imaging Tomography for Gas–Liquid Two-Phase Flow in A Helically Coiled Tube", Measur. Sci. Technol., vol. 16, pp. 1459–1468, 2005.

[16] Paisarn Naphon and Somchai Wongwises,"A Review of Flow and Heat Transfer Characteristics in Curved Tubes", Renewable and Sustainable Energy Reviews, vol. 10(5), pp 463–490, 2006.

[17] Erling Næss, "An Experimental Investigation of Heat Transfer on the Annular Side of Helically Coiled Double Pipe Heat Exchangers", International Conference on Heat Transfer, Fluid Mechanics and Thermodynamics, vol. 6, pp. NE2, 2008.

[18] D. Colorado, J.A. Hernández, O. García-Valladares, A. Huicochea, J. Siqueiros, "Numerical Simulation and Experimental Validation of A Helical Double-Pipe Vertical Condenser", Applied Energy, vol. 88(6), pp. 2136–2145, 2011.

[19] Ahmed Mohamed Elsayed," Heat Transfer In Helically Coiled Small Diameter Tubes For Miniature Cooling Systems", The school of mechanical engineering university of Birmingham Edgbaston, Birmingham, b15 2tt, 2011.

[20] S. A. Nada, W. G. El Shaer, A. S. Huzayyin, "Performance of Multi Tubes in Tube Helically Coiled As A Compact Heat Exchanger", Heat Mass Transfer, Springer, vol. 50(12), December 2014.

[21] G.B. Mhaske and D.D. Palande, "Enhancement of Heat Transfer Rate of Tube in Tube Helical Coil Heat Exchanger", International Journal of Mechanical Engineering, vol. 3(8), pp. 39–45, 2015.

**Nomenclatures**

| | |
|---|---|
| D | Diameter, m |
| d | Diameter, m |
| h | Specific enthalpy, kJ/kg |
| N | Number of the turns of the helically coiled tube |
| p | Pitch of helically coiled tube, m |
| q | Specific heat, kJ/kg |
| S | Spacing of helically coiled tube |
| w | Specific work, kJ/kg |
| **Dimensionless Groups** | |
| De | Dean number |
| Re | Reynolds number |
| **Greek Letters** | |
| δ | Dimensionless coil curvature ratio |
| λ | Coil torsion (dimensionless pitch ratio) |
| **Superscripts and Subscripts** | |
| c | Coil/Condenser |
| ev | Evaporator |
| ref | Refrigerant |
| w | Water |
| **Acronyms and Abbreviations** | |
| COP | Coefficient of Performance |
| HCT | Helically Coiled Tube |
| HCTIT | Helically Coiled Tube-In-Tube |
| PVC | Polyvinyl Chloride |
| RE | Refrigeration Effect |
| VCRS | Vapour Compression Refrigeration System |

**خلاصة البحث**

يتناول هذا البحث دراسة تجريبية للتحقق من تأثير الشكل الهندسى وظروف التشغيل لمبخر على شكل أنبوبة بداخل أنبوبة حلزونية الشكل على معامل أداء دائرة تبريد بإنضغاط البخار. تمت الدراسة على مبخرات فى وضع رأسى ويمر وسيط التبريد (R134a) فى الأنبوبة الداخلية بينما يمر ماء التسخين فى مجراهم الحلقى، وكان الجريان معاكساً. تم تصنيع خمسة ملفات حلزونية بأشكال هندسية مختلفة لإستخدامهم كمبخر فى دائرة التبريد ، وتمت الإختبارات المعملية بتغيير معدل تدفق ماء التسخين. وتم تقسيم الأشكال الهندسية للمبخرات والمكثفات إلى مجموعتين : فى المجموعة الأولى تم تغيير نسبة الإنحناء للأنبوبة الداخلية من ٠,٠٢٣٨ إلى ٠,٠٣٣٤ ، بينما تم فى المجموعة الثانية تغيير نسبة إلتواء اللفات من ٠,٠٥٢٢ إلى ٠,٠٩٤٨ . أظهرت النتائج المعملية أن معامل أداء دائرة التبريد بإنضغاط البخار يتحسن بنقصان نسبة الإنحناء وزيادة نسبة الإلتواء للمبخر و زيادة النسبة بين ضغط المكثف وضغط المبخر. فى نهاية الدراسة تم إستنتاج معادلات إرتباط وذلك لحساب معامل أداء دائرة التبريد بإنضغاط البخار فى مدى المعاملات التى تم دراسة تأثيرها.